Evaluation of spatial hydraulic head distribution using Empirical Bayesian Kriging and ANFIS methods in Dogger Karst Aquifer

Karstik Dogger Akiferi'nde konumsal hidrolik yük dağılımının Ampirik Bayes Kriging ve ANFIS yöntemleriyle değerlendirilmesi

Günseli ERDEM[1,2]* iD, Bedri KURTULUŞ[1,3] iD

[1] *Muğla Sıtkı Koçman University, Geological Engineering Department, 48000 Muğla, Turkey*
[2]*Nişantaşı University, Civil Engineering Department, 34485, Istanbul, Turkey*
[3]*King Fahd University of Petroleum and Minerals, Center for Environment and Water, 31261 Dhahran, Saudi Arabia*

ABSTRACT

In this study, Adaptive Neuro Fuzzy based Inference System (ANFIS) and Empirical Bayesian Kriging (EBK) are evaluated for assessing hydraulic head distribution in a karst aquifer. ANFIS uses three reduced centered preprocessed inputs, which are cartesian coordinates (XY) and the elevation (Z). All models are applied to the same case study: Dogger aquifer, which covers an area of 445 km^2 in the south east of Poitiers, France. Models are tested on 100 random data subset of 20 data among 113, the remaining is used to train and validate the models. ANFIS$_{XYZ}$ and EBK are then used to interpolate the hydraulic head on a 100 m square - grid covering the study area. Both EBK and ANFIS interpolations exhibit similar patterns, with the average values of RMSE = 5.2 m and R^2 = 0.80. Combining these approaches can be an advanced option for interpolating hydraulic head in a more accurate way.

Keywords: ANFIS, Empirical Bayesian Kriging, Hydraulic head, Dogger, Karst, France.

ÖZET

Bu çalışmada, karstik bir akiferdeki hidrolik yük dağılımı, Bulanık mantıklı yapay sinir ağları (ANFIS) ve Ampirik Bayes Kriging (EBK) yöntemleri ile değerlendirilmiştir. ANFIS, önceden elde edilmiş kartezyen koordinatları (XY) ve yükseklik datasını (Z) giriş verisi olarak kullanır. EBK, giriş datalarından birçok semi-variogram modelini tahmin ederek ortaya çıkan hatayı hesaba katar ve enterpolasyonda kullanır. İki yöntem sonucunda çıkan modeller aynı çalışma alanındaki hidrolik yük dağılımını incelemede kullanılmıştır: Dogger akiferi, Fransa'nın Poitiers şehrinin güneydoğusunda yer alır ve 445 km^2 genişliğinde bir alanı kaplamaktadır. Toplam 113 hidrolik yük verisinin içinden 20 verinin 100 adet rastgele veri alt kümesinde test edilerek modeller elde edilmiştir. Geriye kalan veriler ise modelleri eğitmek ve doğrulamak için kullanılmıştır. ANFIS$_{XYZ}$ ve EBK daha sonra çalışma alanını kaplayan 100 m^2 büyüklüğünde alana sahip hücrelere ayrılarak her hücredeki hidrolik yükü enterpole etmek için kullanılmıştır. Hem EBK hem de ANFIS enterpolasyonları, ortalama RMSE = 5.2 m ve R^2 = 0.80 değerleri ile benzer enterpolasyon sonuçları göstermiştir. Bu iki yaklaşımı birleştirmek hidrolik yük dağılımını daha doğru enterpole etmek için gelişmiş bir seçenek olabilir.

Anahtar sözcükler: ANFIS, Ampirik Bayes Kriging, Hidrolik yük, Dogger, Karst, Fransa.

1. INTRODUCTION

Earth scientists (hydrologists, geologists, biogeochemists…) are interested in understanding the behavior of hydro systems (Kurtuluş et al., 2011; Flipo et al., 2012). Experiments and observations were done first in the field at determined locations. These observations and measurements were distributed as timewise and spatially using modelling techniques that are based on several approaches (Amini et al., 2010; Yeganeh et al., 2017). As part of the hydro system, aquifer systems play a decisive role in its behavior and act as a reservoir.

The state of an aquifer unit is characterized by its piezometric head or hydraulic head. The head is measured as the water level in piezometers. The mapping of these punctual data is useful for many environmental applications, such as water resources management. Estimates of the hydraulic head distribution are frequently used to determine the capture zone of pumping wells. Hydraulic head maps are also important tools for earth dam monitoring Rivest et al., 2008). They are also used to initialize distributed models, which are nowadays critical tools for managing water resources at the basin scale (Perkins and Sophocleous, 1999; Flipo et al., 2007; Flipo et al., 2012; Flipo et al., 2014). As reported in (Flipo et al., 2012) many inverse methodologies in hydrogeology use hydraulic head map as a pre-requisite (24 publications among 45). The mapping of hydraulic heads requires synchronous measurements; usually, achieved with synchronous snapshot campaigns. Synchronous snapshot campaigns are feasible for relatively small aquifer units (~100 km^2), such as the Orgeval basin (Kurtuluş et al., 2011, Kurtuluş and Flipo, 2012, Mouhri et al., 2013). The larger the aquifer unit, the longer the measurement campaigns, which can last years for regional aquifer systems (>100000 km^2) (Tóth,

2002) and therefore introduce uncertainties in the final mapping.

Understanding the temporal and spatial variations of the depth to groundwater is a prerequisite to achieve sustainable water use in a basin. Point measurements of water table levels are available, but what is needed are groundwater surfaces based on these measurements. Robust interpolation methods are needed to interpolate hydraulic head point measurements. Many have been discussed in the literature (Kurtuluş *et al.*, 2011).

On the one hand, a technique often used in earth sciences and especially in hydrogeology is kriging (Cressie, 1990; Rouhani and Myers, 1990; Weber and Englung, 1994; Zimmerman et al., 1999; Brochu and Marcotte, 2003; Theodossiou and Latinopoulos, 2006; Lyon *et al.*, 2006; Ahmadi and Sedghamiz, 2007; Abedini *et al.*, 2008; Renard and Jeannée, 2008; Ta'any *et al.*, 2009; Buchanan and Triantafilis, 2009; Pardo-Igúzquiza *et al.*, 2009; Sun *et al.*, 2009; Plouffe *et al.*, 2015). Few authors compared the efficiency of different interpolation techniques with kriging, co-kriging, kriging with external drift (Hoeksema *et al.*, 1989; Boezio *et al.*, 2006; Pardo-Igúzquiza and Chica-Olmo, 2007; Ahmadi and Sedghamiz, 2008; Bargaoui and Chebbi, 2008). Kriging using DEM information as an external drift seems the most efficient methodology for unconfined aquifer units (Desbarats *et al.*, 2002; Rivest *et al.*, 2008), which is in agreement with the high correlation between hydraulic head and soil surface in such systems (Tóth, 1962). Empirical Bayesian Kriging (EBK) has been introduced in the literature for a few years (Pilz and Spöck, 2007; Pilz *et al.*, 2012). EBK automates the selection procedure of valid Kriging models. It uses several semivariogram models rather than a single semivariogram. Finzgar *et al.* (2014) performed a recent study about the spatial distribution of metal contamination using EBK.

On the other hand, hydrologists have started to incorporate fuzzy logic and artificial neural network (ANN) concepts to their methodologies with various identified papers (Maier *et al.*, 2010; Sivapragasam *et al.*, 2014; Kant *et al.*, 2013; Rezaeianzadeh *et al.*, 2014) especially for rainfall-discharge transformation at the catchment scale (Alvisi and Franchini, 2011; Johannet *et al.*, 2007; Kurtuluş and Razack, 2007; Lallahem and Mania, 2003; Minns and Hall, 2004). It was noticed that ANFIS (Takagi and Sugeno, 1985; Jang, 1993; Jang, 1995; Jang, 1996; Celikyilmaz and Turksen, 2009; Wang *et al.*, 2009; Sağır and Kurtuluş, 2017) exhibits better simulation performances than classical artificial neural networks (Nayak *et al.*, 2004; El-Shafie *et al.*, 2007; Fırat, 2008; Pai *et al.*, 2009; Maier et al., 2010). Moreover, ANFIS was already used to interpolate hydraulic head distribution successfully (Lin and Chen, 2004; Kholghi and Hosseini, 2009; Flipo and Kurtuluş, 2011; Kurtuluş *et al.*, 2011; Kurtuluş and Flipo, 2012; Tapoglou *et al.*, 2014).

The goal of this work is to compare the until now best hydraulic head distribution interpolation methods, represented by Empirical Bayesian Kriging (EBK) using two input variables with cartesian coordinates (X,Y) and adaptive neuro fuzzy based inference system (ANFIS) using three input variables: cartesian coordinates associated with DEM (X,Y,Z).

In this paper, the watershed of study and the available dataset are presented. Then presented two different models are tested: ANFIS and EBK. The ANFIS models are built with three inputs for different types of membership function that are reduced and centered variables. The two input model considers just cartesian coordinates for EBK. The three input model uses cartesian coordinates and the elevation of the ground (ANFISxyz). EBK is considered to belong to the two input models, whereas ANFIS belongs to the three input models.

All models are then applied on the same case study: an agricultural basin of the Dogger aquifer covers an area of 445 km²

located south east of Poitiers in France. Models are tested on a subset of 20 data among 113, the remaining is used to train and validate the four different membership function. All models are then used to interpolate the hydraulic head distribution on a 100 m square - grid covering the area of study. Finally, the two best models are retained and the resulting hydraulic heads are compared.

2. MATERIALS AND METHOD

2.1. Experimental Site and Data

The Dogger karstic basin covers an area of 445 km^2 (see Figure 1) and is located 295 km south east from Paris. The average annual air temperature is 11.5 °C. The annual mean rainfall is 687 mm. The hydrological behavior of the Dogger karstic basin is influenced by the unconfined aquifer system, which is composed of one main Mesozoic geological formation: the middle Jurassic – Dogger aged, Callovien limestone, Bathonien white limestone gravel with flint and Bajocien limestone gravel with flint punctuated, crinoidal bioclastic limestone, oolitic and oncolites and dolomitic limestone (see Figure 1) (Le Gal La Salle *et al*., 1996; Riva *et al*., 2009). The Bajocian (103-46 m) consists of bioclastic limestone, which has a fine texture in their basal part (103-91 m) and a granular one (ooids, oncolites, pellets) in the rest of the unit. The granular limestone is interbedded with cherty layers in the upper Bajocian (58-46 m) (Audouin *et al*., 2008). The basin is relatively flat with increasing slopes near to the valley at the river mouth (80 % of the territory spans between 56 and 149 m above mean sea level). This work focuses on hydraulic head distribution in the eastern to the western part of the basin covering the zone between "Le Clain" and "La Vienne" rivers in the North Aquitaine Watershed (see Figure 1). Hydraulic heads were measured in 68 wells and 45 other hydraulic head points on the river (see Figure 1). Totally, the overall dataset is composed of 113 hydraulic heads.

The goal is to determine the hydraulic head distribution of subsurface karst aquifer unit connected to Callovian limestone. Due to the complex geometry of the karst aquifer system at the river part of the North Aquitaine basin, it is necessary to complete the well dataset. For this purpose, a 90 m x 90 m cell sized DEM of the study area was obtained from SRTM data. All the measured well data was located on the DEM for interpolation process.

2.1. Interpolation Methods

2.2.1. Kriging

Geostatistic aims at providing quantitative descriptions of natural variables distributed in space and time (Journel, 1986; Chilès and Delfiner, 1999). Initially developed to address ore reserve evaluation issues in mining (Isaaks and Srivastava, 1989), it is now commonly applied to environmental sciences such as hydrogeology, air, water and soil pollution (Goovaerts, 1997). Geostatistic is used to characterize the spatial structure of the variable of interest by means of a consistent probabilistic model. This spatial structure is characterized by the variogram, which describes how the variability between sampled concentrations increases with the distance between the samples. A variogram model is fitted to the experimental variogram for subsequent analysis. The interpolation technique, known as kriging, provides the "best", unbiased, linear estimate of a regionalized variable at unsampled locations, where "best" is defined in a least squares sense, as it aims to minimize the variance of estimation error (Chilès and Delfiner, 1999). As for the classical interpolations, the estimation by kriging of the concentration at any target cell is obtained by a linear combination of the available sample concentrations. The kriging differentiates only by the way of choosing the coefficients of this linear combination. Those coefficients are called kriging weights and depend on:

- the distances between the data and the target (like other classical interpolators),
- the distances between the original data themselves (data clustering),
- the spatial structure of the variable.

Exploratory data analysis, automatic variogram fitting and kriging are performed using the ArcGIS 10.3.1 software. The basic tool used for kriging is the semivariogram γ (see Equation 1), defined as half the expectancy of deviation between values of samples separated by a distance h. In this case it traduces the spatial variability of the variable Z(x):

$$\gamma(h) = (1/2) * E[(Z(x) - Z(x + h))^2] \qquad (1)$$

where *E[V]* defines the mathematical average of the coordinates of the vector *V*.

Let say, *Z*(x)* is the kriged value at location *x*, $Z(x_i)$ is the known value at location x_l, λ_i is the weight associated with the data, μ is the Lagrange multiplier and $\gamma(x_i\ x_j)$ is the value of variogram corresponding to a vector with origin in x_i, and extremity in x_j The general equation of Kriging estimator is:

$$Z^*(x) = \sum_{t=1}^{n} \lambda_i Z(x_i) \qquad (2)$$

In order to achieve unbiased estimations in kriging and to minimize the variance of estimates the following set of equations should be solved simultaneously (Goovaerts, 1997):

$$\begin{cases} \sum_{i=1}^{N} \lambda_i = 1 \\ \sum_{i=1}^{N} \lambda_j \gamma(\chi_i \chi_j) - \mu = \gamma(\chi_i, \chi), \\ i = 1, 2 \dots N \end{cases} \qquad (3)$$

2.2.2. Empirical Bayesian Kriging

Empirical Bayesian Kriging is a geostatistical interpolation method that automates the difficult aspects of building a valid kriging model. Other kriging methods require to manually adjust parameters, but EBK automatically calculates these parameters through the processes of subsetting and simulations (Chilès and Delfiner, 1999). EBK method can handle moderately nonstationary input data estimates and then uses many semivariogram models rather than a single semivariogram. EBK accounts for the error introduced by estimating the underlying semivariogram through repeated simulations (Finzgar *et al*., 2014).

2.2.3. Adaptive Neuro Fuzzy Inference System

Adaptive neuro-fuzzy inference system (ANFIS) (Firat and Gungor, 2007; Jang, 1993; Jang, 1995; Jang, 1996; Pratihar, 2008; Takagi and Sugeno, 1985; Wang *et al*., 2009; Erdem *et al*., 2016) is a modelling technique which assumes that input and output data are ill-defined with uncertainty that cannot be exactly assessed with probability theory based on a two-valued logic. It uses fuzzy set theory first proposed by Zadeh (1965). A fuzzy set is a set of elements with an imprecise (vague) boundary (Pratihar, 2008). A fuzzy set does not have a crisp boundary. That is, the transition from "belonging to the set" to "not belonging to the set" is gradual and is characterized by membership functions. A fuzzy set *A(x)* is then represented by a pair of two things - the first one is the constituent elements x and their associated membership values *μA(x)* that is their degree of belongingness:

$$A(x) = \{(x, \mu_A(x)), x\epsilon X\} \qquad (4)$$

Where *X* is the Universal set consisting of all possible elements. The membership function *μA* ranges between zero and one. If the value of the membership function is restricted to either zero or one, the fuzzy set is then reduced to classical crisp set with a known boundary. As stated by Jang (1995), the fuzziness does not come from the randomness of the constituent members of the sets, but from the uncertain and imprecise nature of the abstract thoughts and concepts.
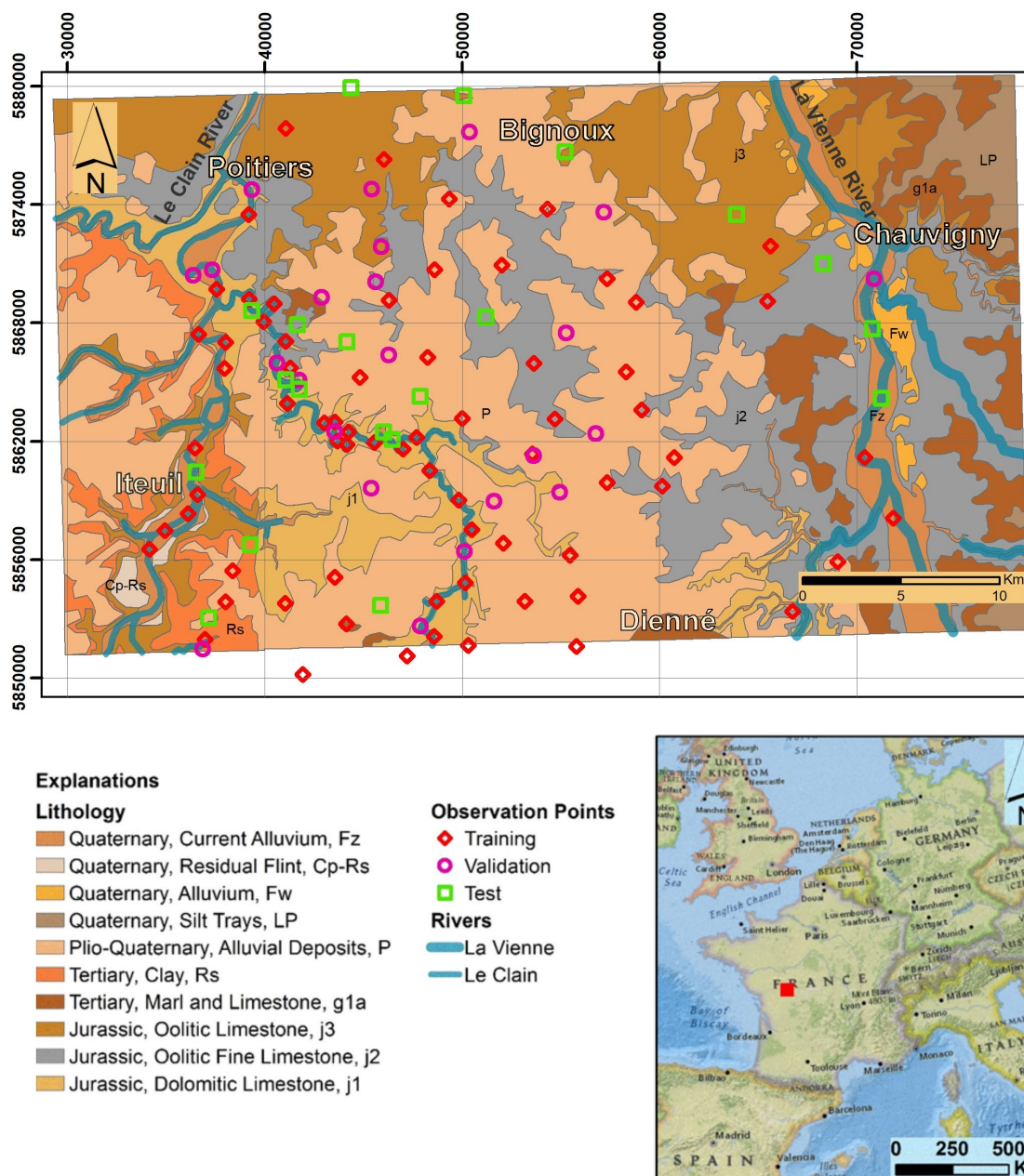
Figure 1. Geological map of North Aquitaine Dogger aquifer (géoportail, BRGM), location of wells and river points divided into training, validation and testing sets (selected in TriMF4).

In ANFIS, the relationship between input and output is expressed in the form of If-Then rules. ANFIS used for the present work is based on Sugeno fuzzy model (Takagi and Sugeno, 1985) which formalizes a systematic approach to generating fuzzy rules from an input-output dataset. A typical fuzzy rule in a Sugeno fuzzy model has the format: If $x \epsilon A$ and $y \epsilon B$ then $z=f(x,y)$, where A and B are fuzzy sets in the antecedent and $f(x,y)$ is a crisp function in the consequent. Usually f is a polynomial function.

The architecture of the ANFIS is composed of five layers (see Figure 2). Each layer has a specific function. The first layer generates a membership grades of a linguistic label. It means that it defines the parameter of the

membership functions.
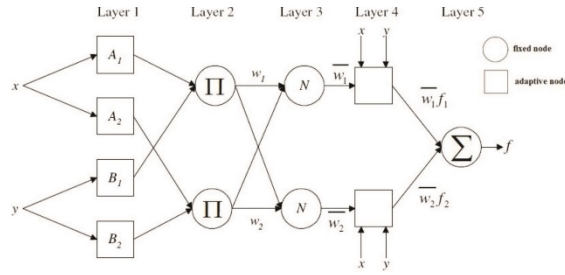
Figure 2. ANFIS architecture for three inputs x, y, z; Layer 1: generates membership grades; Layer 2: Fuzzy rules; Layer 3: calculates weights or rules named firing strengths; Layer 4: product of the normalized firing strengths; Layer 5: Fuzzy results transformed into a traditional output by summation.

For instance, let consider a first order Sugeno fuzzy inference system which contains two rules (see Equation 5 and 6):

Rule 1: If $X \epsilon A_1$ and $Y \epsilon B_1$ then:

$$f_1 = p_1 x + q_1 y + r_1; \qquad (5)$$

Rule 2: If $X \epsilon A_2$ and $Y \epsilon B_2$ then:

$$f_2 = p_2 x + q_2 y + r_2; \qquad (6)$$

$p_1, q_1, r_1, p_2, q_2, r_2$ are defined in the first layer of the ANFIS (see Figure 2).
Each node i of layer two calculates the firing strength w_1 of the ith rule via multiplication (see Equation 7)

$$w_1 = \mu_{A_1}(x)\mu_{B_1}(y) \qquad (7)$$

Node i in the layer three calculates the ratio of the ith rule's firing strength to the total amount of all firing strengths (see Equation 8):

$$\overline{W_1} = W_1/(\sum_j W_j) \qquad (8)$$

Node i in the layer four calculates the contribution (weight) of the ith rule toward the overall output via multiplication (see Equation 9):

$$\overline{W_i} = \overline{W_i} f_i \qquad (9)$$

Finally, layer five is made on a single node that computes the overall output as the summation of the contribution from each rule (see Equation 10):

$$f(x, y) = \sum_i \overline{W_i} = \sum_i \overline{W_i} f_i \qquad (10)$$

ANFIS uses a hybrid learning algorithm that combines the back-propagation gradient descent and least squares methods to create a fuzzy inference system whose membership functions are iteratively adjusted according to a given set of input and output data (Jang, 1993). For each iteration, the back-propagation method involves minimization of an objective function using the steepest gradient descent approach in which the network weights and biases are adjusted by moving a small step in the direction of a negative gradient. The iterations are repeated until a convergence criterion or a specified number of iterations is achieved. It has the advantage of allowing the extraction of fuzzy rules from numerical data and adaptively constructs a rule base.

2.3. Model Implementation

2.3.1. Implementation of Empirical Bayesian Kriging

EBK method is based on three main steps: Firstly, a semi-variogram model is estimated from the observed data set. Secondly, a new value is simulated at each of the observed data locations by using the semi-variogram estimated on the previous step. Thirdly, a new semi-variogram model is estimated from the newly simulated data at the second step. By using Bayes' rule, a value of weight for this semi-variogram model is calculated which shows how likely the observed data can be generated from the semi-variogram. The second and third steps are repeated. This process creates a spectrum of semi-variograms (Pilz and Spöck, 2007). New parameters are needed also for EBK such as; subset size which defines the number of points in each subset; overlap factor which specifies the degree of

overlap between subsets and number of simulation which specifies the number of semi-variogram that will be simulated for each subset.

2.3.2. Implementation of Adaptive Neuro Fuzzy Inference System

The neuro fuzzy model was developed using the ANFIS procedures of MATLAB (Demuth and Beale, 2003). In this study, a code is written in Matlab 2012b for ANFIS using appropriate functions to calculate the best performance of the methods.

Before using the model to interpolate unknown outputs (hydraulic head), its actual predictive performance must be tested by comparing outputs estimated by calibrated models with known outputs. At each phase (training, validation and test), the ANFIS performance is measured by the determination of the coefficient of goodness-of-fit (R^2) and the root mean square error (RMSE) (see Equation 11).

$$RMSE = \sqrt{E\left[\left(Z^*(x) - Z(x)\right)^2\right]} \qquad (11)$$

where E, Z^* and Z are previously defined (section 2.2.1).

Input data are XY coordinates and the ground elevations of piezometers for ANFIS$_{XYZ}$. The data are pre-processed by the elimination of unrealistic values to obtain more stable dataset. Hydraulic head is the ANFIS output.

The selection of appropriate input parameters is a complex task. At first step; numbers of training, validation and test data are decided by order: 70 (62 %), 23 (20 %) and 20 (18 %). Assignment of data points to training, validation and test subsets is realized by random selection ability of ANFIS. Triangular, Gaussian, Generalized bell, Spline-based, Trapezoidal and their different types of curves (named as 2, 3 and 4) are used as membership functions in ANFIS. Random simulation number is decided as 100 which provides 100 different data assignments to training, validation and test subsets for each type of membership

function. For ANFIS$_{XYZ}$ simulations, the number of rules is set to three for each input.

2.4. Selection of Interpolation Models

2.4.1. EBK Process

In order to achieve more realistic interpolation, hydraulic head values are not directly used as input of EBK. Firstly, depths from the ground to water level are calculated for each observation point of hydraulic head. These depth values are interpolated by EBK (see Figure 3). For the creation of semi-variogram cloud in EBK; subset size, overlap factor, number of simulations, maximum neighbors, minimum neighbors and radius (m) are determined by order: 65, 2, 100, 50, 25 and 5000. The obtained result raster data of depth interpolation is subtracted from DEM raster to derive the hydraulic head raster. By this way, the encountered error which comes from EBK method is minimized.

2.4.2. ANFIS Model Selection

The ANFIS model selection is based on available data. Using these datasets at each phase (training, validation and test), the ANFIS performance is measured by the coefficient of goodness-of-fit (R^2) and root mean square error (RMSE). ANFISXYZ is run up to 2000 iterations with 100 random data simulations for three types of each membership function. One hundred results for each type of membership functions are analyzed automatically to select the best ones. RMSE and R^2 values of training, validation and test subsets for the best types of membership functions are given in Table 1. In this table, according to the RMSE and R2 training and validation values, TriMF4, GaussMF4, GbellMF3, PiMF2 and TrapMF4 are picked out as the best types in their membership functions (see Figure 4). The best model can be considered as TriMF4 for RMSE and R^2 values are 3.6 m and 0.96 respectively. General descriptive statistics and R^2 values of all ANFIS membership function types and EBK results are given in Table 2.
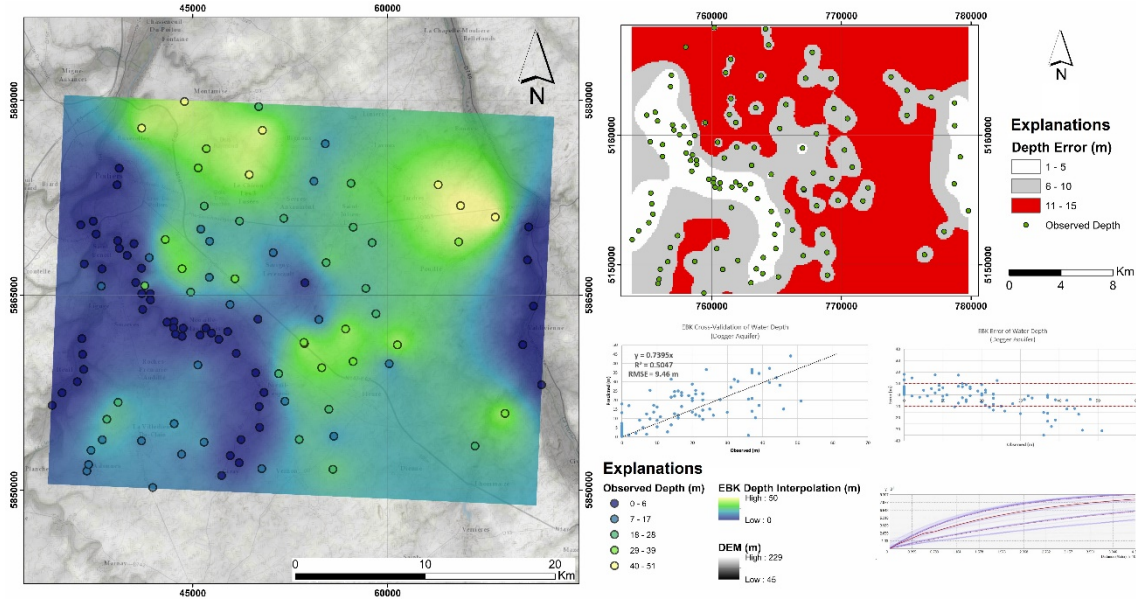
Figure 3. EBK interpolation, standard error, cross validation, error graph and semi-variogram cloud of depth to water.

Table 1. RMSE and R^2 values of training, validation and test subsets for the best types. of membership functions.

Member-ship Function	Member-ship Function Type	Number of Simulation	Number of Iteration	RMSE Training (m)	RMSE Validation (m)	RMSE Test (m)	R^2 Training	R^2 Validation	R^2 Test
TriMF	2	58	2000	3.1	6.8	6.4	0.96	0.72	0.81
	3	94	2000	0.0	4.5	4.9	1.00	0.90	0.86
	4	40	2000	0.0	4.0	3.6	1.00	0.91	0.96
GaussMF	2	73	2000	2.2	3.2	7.1	0.97	0.94	0.81
	3	54	2000	0.0	7.8	6.1	1.00	0.76	0.83
	4	49	2000	0.0	4.5	4.7	1.00	0.90	0.91
GbellMF	2	87	2000	1.1	7.0	4.6	0.98	0.80	0.90
	3	40	2000	0.0	5.4	4.2	1.00	0.82	0.89
	4	20	2000	0.0	4.3	5.4	1.00	0.92	0.82
PiMF	2	28	2000	2.1	5.7	3.5	0.97	0.85	0.94
	3	49	2000	0.0	5.8	4.3	1.00	0.82	0.92
	4	34	2000	0.0	4.7	4.3	1.00	0.87	0.93
TrapMF	2	47	2000	1.5	6.9	5.8	0.99	0.68	0.89
	3	98	2000	0.0	4.2	6.1	1.00	0.91	0.87
	4	73	2000	0.0	3.0	4.5	1.00	0.95	0.93

Table 2. General descriptive statistics and R^2 values between each other of all ANFIS membership function types and EBK results.

	R^2 (vs. Observed)	Mean (m)	Median (m)	Standard Deviation (m)	Kurtosis	Skewness	Minimum (m)	Maximum (m)	CV
Observed	-	96.96	98.74	14.70	-0.88	-0.38	65.45	123.08	0.15
EBK	0.51	97.70	99.62	14.88	-0.84	-0.44	63.51	122.86	0.15
TriMF2	0.75	99.17	102.54	11.90	-0.25	-0.76	64.96	118.34	0.12
TriMF3	0.89	98.36	101.01	14.29	-0.36	-0.54	63.38	124.13	0.15
TriMF4	0.86	98.12	101.06	14.28	-0.62	-0.59	64.49	120.79	0.15
GaussMF2	0.84	98.22	101.70	13.45	-0.28	-0.84	62.89	117.50	0.14
GaussMF3	0.82	97.39	99.56	13.41	-0.56	-0.64	65.92	116.62	0.14
GaussMF4	0.82	97.32	98.60	14.62	-0.61	-0.43	65.66	124.68	0.15
GbellMF2	0.80	98.99	100.82	12.94	0.43	-0.73	53.57	122.86	0.13
GbellMF3	0.78	97.77	100.98	13.51	-0.59	-0.57	65.87	121.39	0.14
GbellMF4	0.85	97.33	99.01	15.84	-0.47	-0.14	62.62	138.21	0.16
PiMF2	0.76	98.05	101.15	12.06	-0.53	-0.44	67.84	121.67	0.12
PiMF3	0.84	97.47	100.24	15.11	0.37	-0.79	43.26	124.03	0.16
PiMF4	0.84	98.42	100.72	14.22	-0.28	-0.67	63.78	120.90	0.14
TrapMF2	0.74	98.81	101.96	13.44	-0.28	-0.73	58.22	119.03	0.14
TrapMF3	0.82	98.55	101.73	14.82	-0.32	-0.65	54.65	124.13	0.15
TrapMF4	0.86	98.39	102.13	13.64	-0.42	-0.70	65.41	118.98	0.14

2.4.3. Testing of Models

All model results of ANFIS and EBK interpolation are assessed together based on R^2 and descriptive statistics (Table 2). The performance of ANFIS models are slightly better than EBK. R^2 between EBK and observed value is 0.50 whereas the best R^2 between ANFIS and observed value is 0.89 (TriMF3) (Table 2). TriMF4 is decided as the best ANFIS result according to the evaluation of R^2, descriptive statistics and the prediction of hydraulic head map pattern. The difference map between EBK and the best selected ANFIS model is given in Figure 5. Except for the east and the west of this map, the difference between EBK and ANFIS is calculated up to 10 meters
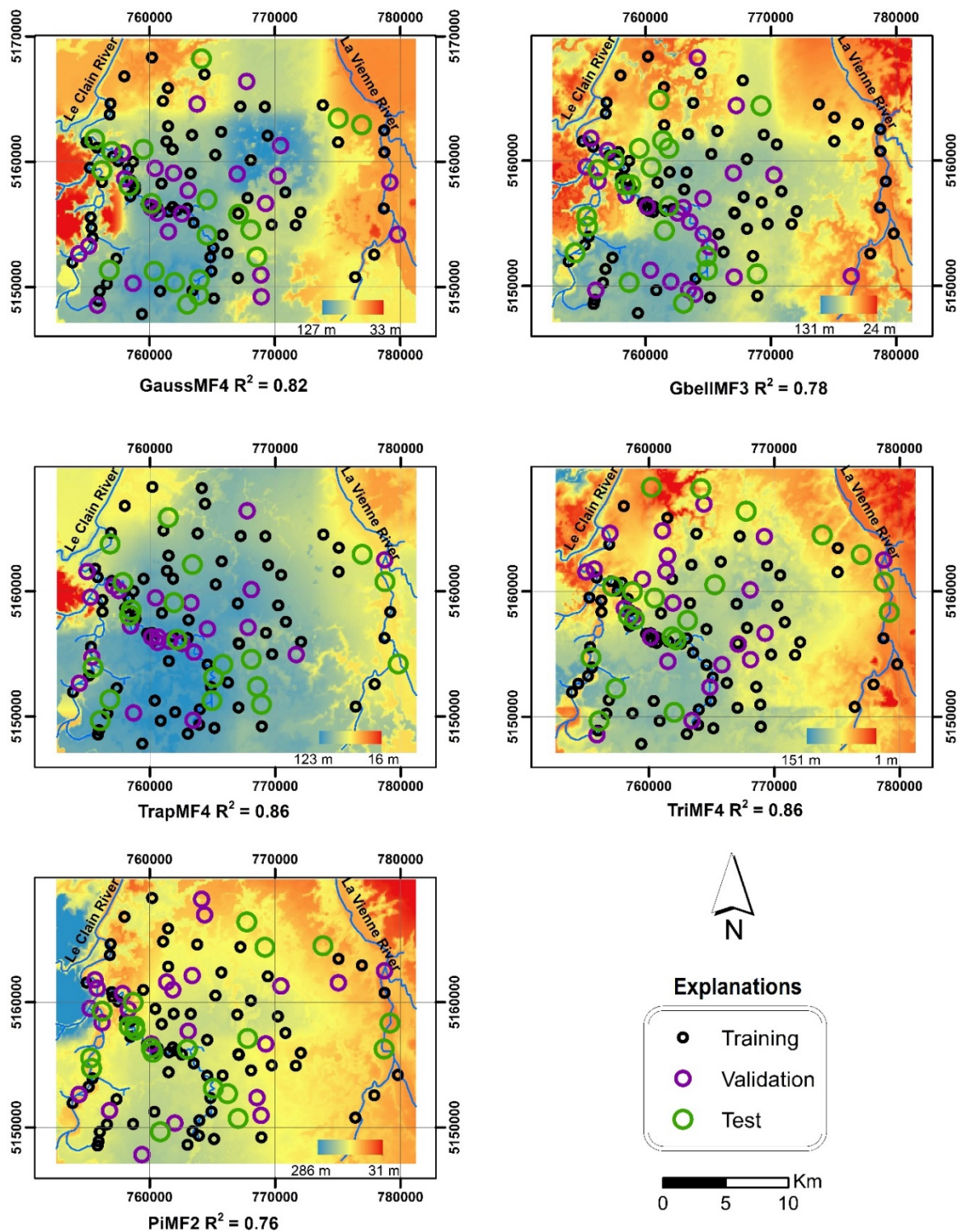
Figure 4. Best simulation maps of each ANFIS membership function and random data selections of them.
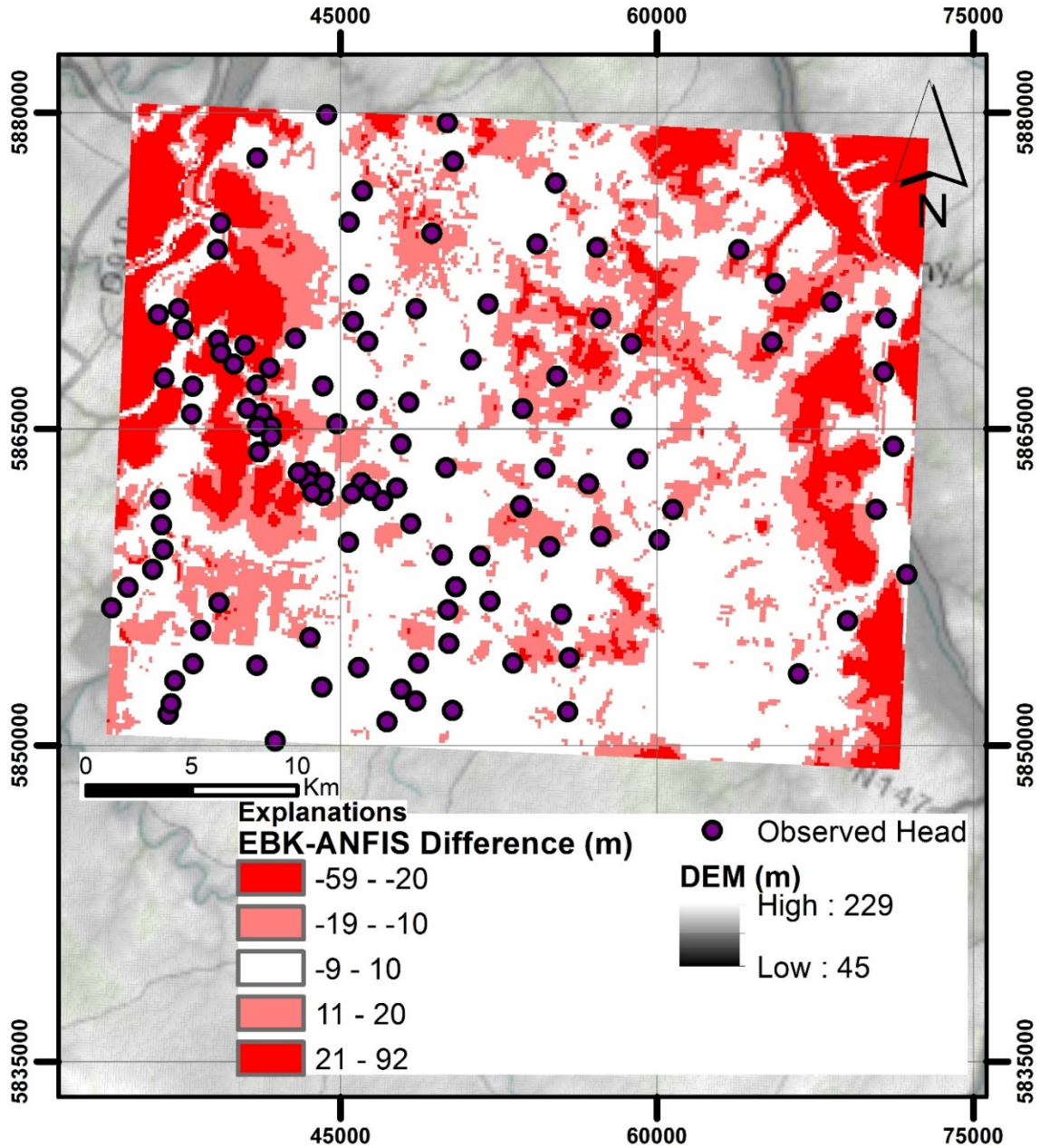
Figure 5. The difference map between EBK and ANFIS (TriMF4) hydraulic head predictions.

3. RESULTS

For each model (all membership types of ANFIS and EBK) the hydraulic head distribution was calculated on a 100 m square grid. In ANFIS, observed hydraulic head parameters were directly used as input. But in EBK, hydraulic head interpolation was obtained through the water depth interpolation. Generally, ANFIS models produced less dispersed values with standard

deviations between 11.90 m and 15.84 m while standard deviations of EBK and observed data are 14.88 m and 14.70 m. In terms of statistics (minimum, maximum, mean and standard deviation), ANFIS results are more consistent with the observed parameters (Table 2).

ANFIS (TriMF4) and EBK prediction maps are given in Figure 6. The lowest hydraulic head value in ANFIS prediction is suspiciously one meter while the lowest

value 29 m in EBK prediction can be considered more realistic. The patterns of prediction maps of these two methods do not represent smoothed patterns compare to widespread all other interpolation methods. With the intent to see the predicted hydraulic head values which are greater than ground elevation, predictions of EBK and ANFIS are subtracted from DEM (see Figure 7). In Fig. 7, it can be observed that the red color values do not always represent the error because of the river. It can be also observed that when the DEM is subtracted ANFIS and EBK prediction maps, the difference has larger values around to the rivers
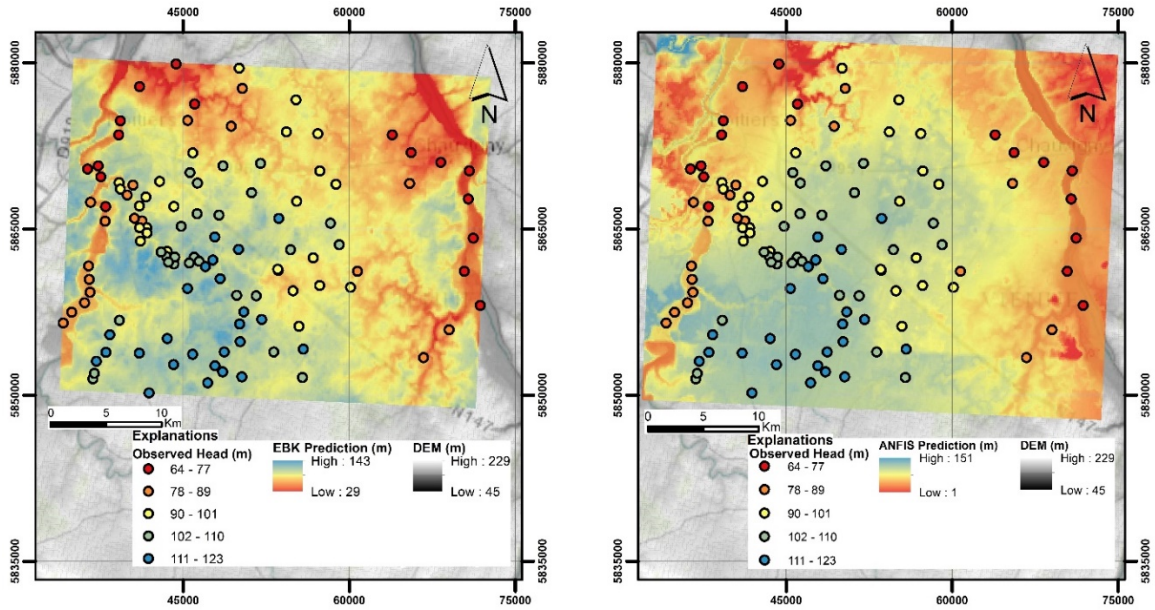
Figure 6. EBK and ANFIS (TriMF4) hydraulic head prediction maps.
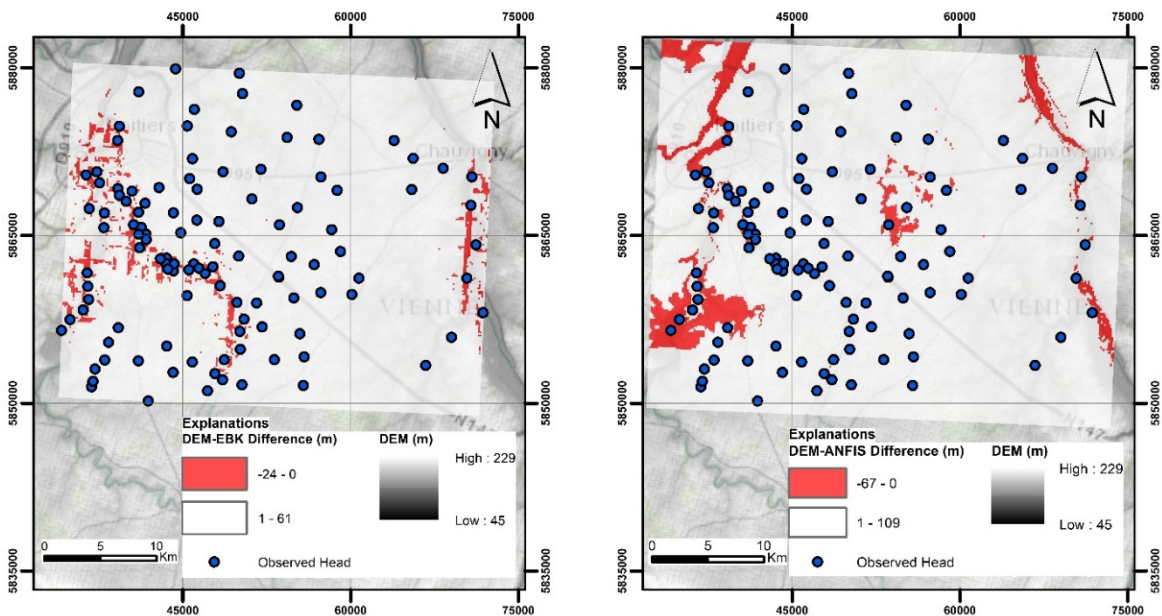
Figure 7. Subtraction maps of EBK and ANFIS (TriMF4) from DEM.

4. DISCUSSIONS

In this paper, two interpolation methods were tested to estimate the hydraulic head distribution over the North Aquitaine Basin of Dogger karstic aquifer. ANFIS was used with three inputs (cartesian coordinates, elevation of the ground and hydraulic head) to interpolate hydraulic head of the study area. The depth values from the ground to water level were used as input of EBK to minimize error for hydraulic head prediction. Hydraulic head distribution results with EBK and ANFIS show that both results are consistent with the topography of the study area. ANFIS and EBK also show that they can accurately predict the real and potential river flow paths. TriMF4 function can be considered as the best result according to its observation vs predicted R^2 = 0.86 for ANFIS while EBK has 0.50 R^2 value compared with observation vs. predicted values.

On the other hand, across the river and unobserved points of the study area, both interpolators are estimated hydraulic heads with different distribution patterns (see Figure 5). For instance, in the west of River Le Clain and in the east of River La Vienne, EBK and ANFIS interpolation values differ up to 92 m. It can be concluded that the reasons for these discrepancies might be the lack of data set and/or complex hydrogeological structure in these areas.

5. CONCLUSIONS

In conclusion, ANFIS can be considered that it gives more realistic results than EBK. However, EBK also proved its efficiency and applicability as an alternative method to interpolate hydraulic head. Surely EBK should also be compared with other kriging methods in the interpolation of hydraulic head (Li and Heap, 2014) ANFIS shows its robustness on hydraulic head prediction where EBK fails to estimate. The advantages of these methods to map hydraulic head distribution are that they minimize the error, give more accurate results than other interpolation methods and require minimal expert knowledge.

DISCLOSURE STATEMENT

The authors declare that there is no conflict of interest.

ORCID IDs

Günseli ERDEM:
https://orcid.org/0000-0002-4061-4336
Bedri KURTULUŞ:
https://orcid.org/0000-0001-6646-9280

6. REFERENCES

Kurtulus, B., Flipo, N., Goblet, P., Vilain, G., Tournebize, J., Tallec, G., (2011). Hydraulic head interpolation in an aquifer unit using anfis and ordinary kriging. In: Madani K et al. (eds) Computational intelligence. 1st edn,. P. 265–276. Berlin, Heidelberg, Springer. https://doi.org/10.1007/978-3-642-20206-3_18.

Flipo, N., Monteil, C., Poulin, M., Fouquet, C., Krimissa, M., (2012). Hybrid fitting of a hydrosystem model: Long term insight into the Beauce aquifer functioning (France). Water Resources Research 48(5). https://doi.org/10.1029/2011WR011092.

Amini, M., Abbaspour, K.C., Johnson, C.A., (2010). A comparison of different rule-based statistical models for modeling geogenic groundwater contamination. *Environmental Modelling & Software* 25(12): 1650-1657. https://doi.org/10.1016/j.envsoft.2010.05.014.

Yeganeh, B., Hewson, M.G., Clifford, S., Knibbs, L.D., Morawska, L., (2017). A satellite-based model for estimating PM2.5 concentration in a sparsely populated environment using soft computing techniques. *Environmental Modelling & Software* 88: 84-92, https://doi.org/10.1016/j.envsoft.2016.11.017.

Rivest, M., Marcotte, D., Pasquier, P., (2008). Hydraulic head field estimation using kriging with an external drift: A way to consider conceptual model information. *Journal of Hydrology* 361(3): 349–361. https://doi.org/10.1016/j.jhydrol.2008.08.006.

Perkins, S.P., Sophocleous, M., (1999). Development of a comprehensive watershed model applied to study stream yield under drought conditions. *Ground Water* 37(3): 418–426. https://doi.org/10.1111/j.1745-6584.1999.tb01121.x.

Flipo, N., Jeannée, N., Poulin, M., Even, S., Ledoux, E., (2007). Assessment of nitrate pollution in the Grand Morin aquifers (France): Combined use of geostatistics and physically-based modeling. Environmental Pollution 146(1):241–256. https://doi.org/10.1016/j.envpol.2006.03.056.

Flipo, N., Mourhi, A., Labarthe, B., Biancamaria, S., Rivière, A., Weill, P., (2014). Continental hydrosystem modelling : the concept of nested stream-aquifer interfaces. Hydrology and Earth System Sciences 18(8)3121–3149. doi:10.5194/hess-18-3121-2014.

Kurtulus, B., Flipo, N., (2012). Hydraulic head interpolation using anfis - model selection and sensitivity analysis. *Computer & Geosciences* 38(1): 43–51, https://doi.org/10.1016/j.cageo.2011.04.019.

Mouhri, A., Flipo, N., Rejiba, F., Fouquet, C., Bodet, L., Goblet, P., Kurtulus, B., Ansart, P., Tallec, G., Durand, V., Jost, A., (2013). Designing a multi-scale sampling system of stream-aquifer interfaces in a sedimentary basin. *Journal of Hydrology* 504: 194–206, https://doi.org/10.1016/j.jhydrol.2013.09.036.

Tóth, J., (2002). József Tóth: An autobiographical sketch. *Ground Water* 40(3): 320–324. https://doi.org/10.1111/j.1745-6584.2002.tb02661.x.

Cressie, N., (1990). The origins of kriging. *Mathematical Geology* 22(2): 239–252, https://doi.org/10.1007/BF00889887.

Rouhani, S., Myers, D.E., (1990). Problems in space-time kriging of geohydrological data. *Mathematical Geology* 22(5): 611–623, https://doi.org/10.1007/BF00890508.

Weber, D.D., Englung, E.J., (1994). Evaluation and comparison of spatial interpolators II. *Mathematical Geology* 26: 589–604, https://doi.org/10.1007/BF02089243.

Zimmerman, D., Pavlik, C., Ruggles, A., Armstrong, M.P., (1999). An experimental comparison of ordinary and universal kriging and inverse distance weighting. *Mathematical Geology* 31(4): 375–390, https://doi.org/10.1023/A:1007586507433.

Brochu, Y., Marcotte, D., (2003). A simple approach to account for radial flow and boundary conditions when kriging hydraulic head fields for confined aquifers. *Mathematical Geology* 35(2): 111–139, https://doi.org/10.1023/A:1023231404211.

Theodossiou, N., Latinopoulos, P., (2006). Evaluation and optimisation of groundwater observation networks using the kriging methodology. *Environmental Modelling & Software* 21(7): 991–1000, https://doi.org/10.1016/j.envsoft.2005.05.001.

Lyon, S.W., Seibert, J., Lembo, A.J., Walter, M.T., Steenhuis, T.S., (2006) Geostatistical investigation into the temporal evolution of spatial structure in a shallow water table. *Hydrology and Earth System Sciences* 10: 113–125.

Ahmadi, S.H., Sedghamiz, A., (2007). Geostatistical analysis of spatial and temporal variations of groundwater level. *Environmental Monitoring and Assessment* 129(1-3): 277–294, https://doi.org/10.1007/s10661-006-9361-z.

Abedini, M.J., Nasseri, M., Ansari, A., (2008). Cluster-based ordinary kriging of piezometric head in West Texas/New Mexico - Testing of hypothesis. *Journal of Hydrology* 351(3): 360–367, https://doi.org/10.1016/j.jhydrol.2007.12.030.

Renard, F., Jeannée, N., (2008). Estimating transmissivity fields and their influence on flow and transport: The case of Champagne mounts. *Water Resources Research* 44(11): 1–12, https://doi.org/10.1029/2008WR007033.

Ta'any, R.A., Tahboub, A.B., Saffarini, G.A., (2009). Geostatistical analysis of spatiotemporal variability of groundwater level fluctuations in Amman-Zarqa basin, Jordan: A case study. *Environmental Geology* 57(3): 525–535, https://doi.org/10.1007/s00254-008-1322-0.

Buchanan, S., Triantafilis, J., (2009). Mapping water table depth using geophysical and environmental variables. *Ground Water* 47(1): 80–96, https://doi.org/10.1111/j.1745-6584.2008.00490.x.

Pardo-Igúzquiza, E., Chica-Olmo, M., Garcia-Soldado, M.J., Luque-Espinar, J.A., (2009). Using semivariogram parameter uncertainty in hydrogeological applications. *Ground Water* 47(1): 25–34, https://doi.org/10.1111/j.1745-6584.2008.00494.x.

Sun, Y., Kang, S., Li, F., Zhang, L., (2009). Comparison of interpolation methods for depth to groundwater and its temporal and spatial variations in the Minqin oasis of northwest China. *Environmental Modelling & Software* 24(10): 1163–1170, https://doi.org/10.1016/j.envsoft.2009.03.009

Plouffe, C.C., Robertson, C., Chandrapala, L., (2015). Comparing interpolation techniques for monthly rainfall mapping using multiple evaluation criteria and auxiliary data sources: A case study of Sri Lanka. *Environmental Modelling & Software* 67: 57-71,https://doi.org/10.1016/j.envsoft.2015.01.011.

Hoeksema, R.J., Clapp, R.B., Thomas, A.L., Hunley, A.E., Farrow, N.D., Dearstone, K.C., (1989) Cokriging model for estimation of water table estimation. *Water Resources Research* 25(3): 429–438, https://doi.org/10.1029/WR025i003p00429.

Boezio, M., Costa, J., Koppe, J., (2006), Accounting for extensive secondary information to improve watertable mapping. *Natural Resources Research* 15(1): 33–48, https://doi.org/10.1007/s11053-006-9014-5.

Pardo-Igúzquiza, E., Chica-Olmo, M., (2007). KRIGRADI: A cokriging program for estimating the gradient of spatial variables from sparse data. *Computers & Geosciences* 33(4): 497–512, https://doi.org/10.1016/j.cageo.2006.08.004.

Ahmadi, S.H., Sedghamiz, A., (2008). Application and evaluation of kriging and cokriging methods on groundwater depth mapping. *Environmental Monitoring and Assessment* 138(1): 357–368, https://doi.org/10.1007/s10661-007-9803-2.

Bargaoui, Z.K., Chebbi, A., (2008). Comparison of two kriging interpolation methods applied to spatiotemporal rainfall. *Journal of Hydrology* 365(1): 56-73, https://doi.org/10.1016/j.jhydrol.2008.11.025.

Desbarats, A.J., Logan, C.E., Hinton, M.J., Sharpe, D.R., (2002). On the kriging of water table elevations using collateral information from a digital elevation model. *Journal of Hydrology* 255(1): 25–38, https://doi.org/10.1016/S0022-1694(01)00504-2.

Tóth, J., (1962). A theory of groundwater motion in small drainage basins in Central Alberta, Canada. *Journal of Geophysical Research* 67(11): 4375–4387, https://doi.org/10.1029/JZ067i011p04375.

Pilz, J., Spöck, G., (2007). Why do we need and how should we implement Bayesian Kriging methods. *Stochastic Environmental Research and Risk Assessment* 22(5): 621-632, https://doi.org/10.1007/s00477-007-0165-7.

Pilz, J., Kazianka, H., Spöck, G., (2012). Some advances in Bayesian spatial prediction and sampling design. *Spatial Statistics* 1: 65-81, https://doi.org/10.1016/j.spasta.2012.03.003.

Finzgar, N., Jez, E., Voglar, D., Lestan, D., (2014). Spatial distribution of metal contamination before and after remediation in the Meza Valley, Slovenia. *Geoderma* 217-218: 135-143, https://doi.org/10.1016/j.geoderma.2013.11.011.

Maier, H.R., Jain, A., Dandy, G.C., Sudheer, K.P., (2010). Methods used for the development of neural networks for the prediction of water resource variables in river systems: Current status and future directions. *Environmental Modelling & Software* 25(8):891–909, https://doi.org/10.1016/j.envsoft.2010.02.003.

Sivapragasam, C., Vanitha, S., Muttil, N., Suganya, K., Suji, S., Selvi, M.T., Selvi, R., Sudha, S.J., (2014). Monthly flow forecast for Missisipi River basin using artificial neural networks. *Neural Computing and Applications* 24(7-8): 1785-1793, https://doi.org/10.1007/s00521-013-1419-6.

Kant, A., Suman, P.K., Giri, B.J., Tiwari, M.K., Chatterjee, C., Nayak, P.C., Kumar, S., (2013). Comparison of multi-objectie evolutionary neural network, adaptive neuro-fuzzy inference system and bootstrap-based neural network for flood forecasting. *Neural Computing and Applications* 23(1): 231-246, https://doi.org/10.1007/s00521-013-1344-8.

Rezaeianzadeh, M., Tabari, H., Yazdi, A.A., Isik, S., Kalin, L., (2014). Flood flow forecasting using ANN, ANFIS and regression models. *Neural Computing and Applications* 25(1): 25-37, https://doi.org/10.1007/s00521-013-1443-6.

Alvisi, S., Franchini, M., (2011). Fuzzy neural networks for water level and discharge forecasting with uncertainty. *Environmental Modelling & Software* 26(4): 523-537, https://doi.org/10.1016/j.envsoft.2010.10.016.

Johannet, A., Ayral, P. & Vayssade, B., (2007). Modelling non measurable processes by neural networks: Forecasting underground flow case study of the Ceze basin (Gard - France). In: "Advances and innovation in systems, computing sciences and software engineering", 1st edn., (K. Elleithy ed.), Springer, pp. 53–58, Dordrecht, https://doi.org/10.1007/978-1-4020-6264-3_10.

Kurtulus, B., Razack, M., (2007). Evaluation of the ability of an artificial neural network model to simulate the input-output responses of a large karstic aquifer, The La Rochefoucauld (Charente, France). *Hydrogeology Journal* 15(2): 241–254, https://doi.org/10.1007/s10040-006-0077-5.

Lallahem, S., Mania, J., (2003). A nonlinear rainfall-runoff model using neural network technique: example in fractured porous media. *Mathematical and Computer Modelling* 37(9-10): 1047–1061, https://doi.org/10.1016/S0895-7177(03)00117-1.

Minns, A. & Hall, M., (2004). Rainfall-runoff modelling. In: "Neural Networks For Hydrological Modeling", 1st edn., (R. Abrahart et al. eds.), CRC Press, pp. 157–176, Leiden.

Takagi, T.M., Sugeno, M., (1985). Fuzzy identification of systems and its applications to modeling and control. *IEEE Transactions on Systems, Man Cybernetics* 15(1): 116–132, https://doi.org/10.1016/B978-1-4832-1450-4.50045-6.

Jang, J.S.R., (1993). ANFIS adaptive-network-based fuzzy inference system. *IEEE Transactions on Systems, Man Cybernetics* 23(3): 665–685, https://doi.org/10.1109/21.256541.

Jang, J.S.R., (1995). Neuro-fuzzy modeling and control. *Proc. IEEE* 83(3): 378–406, https://doi.org/10.1109/5.364486.

Jang, J.S.R., (1996). Input selection for anfis learning. *Proc IEEE Int Conf on Fuzzy Syst.* 2(3): 1493–1499, https://doi.org/10.1109/FUZZY.1996.552396.

Celikyilmaz, A., Turksen, I.B. (2009). *Modeling Uncertainty with Fuzzy Logic*, Berlin, Springer Heidelberg, https://doi.org/10.1007/978-3-540-89924-2

Wang, W.C., Chau, K.W., Cheng, C.T., Qiu, L., (2009). A comparison of performance of several artificial intelligence methods for forecasting monthly discharge time series. *Journal of Hydrology* 374(3): 294–306, https://doi.org/10.1016/j.jhydrol.2009.06.019.

Sağir, Ç., Kurtuluş, B., (2017). Hydraulic head and groundwater 111 Cd content interpolations using empirical Bayesian kriging (EBK) and geo-adaptive neuro-fuzzy inference system (geo-ANFIS). *Water SA* 43(3): 509-519, http://dx.doi.org/10.4314/wsa.v43i3.16.

Nayak, P.C., Sudheer, K.P., Ragan, D.M., Ramasastri, K.S., (2004). A neuro-fuzzy computing technique for modeling hydrological time series. *Journal of Hydrology* 291(1): 52–66, https://doi.org/10.1016/j.jhydrol.2003.12.010.

El-Shafie, A., Taha, M.R., Noureldin, A., (2007) A neuro-fuzzy model for inflow forecasting of the Nile river at Aswan high dam. *Water Resources Management* 21(3): 533–556, https://doi.org/10.1007/s11269-006-9027-1.

Fırat, M., (2008). Comparison of artificial intelligence techniques for river flow forecasting. *Hydrology and Earth System Sciences* 12(1): 123–139.

Pai, T.Y., Wan, T.J., Hsu, S.T., Chang, T.C., Tsai, Y.P., Lin, C.Y., Hu, H.C., Yu, L.F., (2009). Using fuzzy inference system to improve neural network for predicting hospital wastewater treatment plant effluent. *Computers &Chemical Engineering* 33(7): 1272–1278, https://doi.org/10.1016/j.compchemeng.2009.02.004.

Lin, G.F., Chen, L.H., (2004). A spatial interpolation method based on radial basis function networks incorporating a semivariogram model. *Journal of Hydrology* 288(3): 288–298, https://doi.org/10.1016/j.jhydrol.2003.10.008.

Kholghi, M., Hosseini, S.M., (2009). Comparison of groundwater level estimation using neuro-fuzzy and ordinary kriging. *Environmental Modelling & Assessment* 14(6): 729–737, https://doi.org/10.1007/s10666-008-9174-2.

Flipo, N., Kurtulus, B., 2011. Geo-Anfis: Application to piezometric head interpolation in unconfined aquifer unit. Proceedings of the FUZZYSS'11 Congress, November 2011, pp. 195-198, Ankara, Turkey.

Tapoglou, E., Karatzas, G.P., Trichakis, I.C., Varouchakis, E.A., (2014). A spatio-temporal hybrid neural network kriging model for groundwater level simulation. *Journal of Hydrology* 519: 3193-3203, https://doi.org/10.1016/j.jhydrol.2014.10.040.

Le Gal La Salle, C., Marlin, C., Savoye, S., Fontes, J.C., (1996). Geochemistry and 14C dating of ground waters from Jurassic aquifers of North Aquitaine Basin (France). *Applied Geochemistry* 11(3): 433-445, https://doi.org/10.1016/0883-2927(96)00016-9.

Riva, M., Guadagnini, A., Bodin, J., Delay, F., (2009). Characterization of the hydrogeological experimental site of Poitiers (France) by stochastic well testing analysis. *Journal of Hydrology* 369(1): 154-164, https://doi.org/10.1016/j.jhydrol.2009.02.040.

Audouin, O., Bodin, J., Porel, G., Bourbiaux, B., (2008). Flowpath structure in a limestone aquifer: multi-borehole logging investigations at the hydrogeological experimental site of Poitiers, France. *Journal of Hydrology* 16(5): 939-950, https://doi.org/10.1007/s10040-008-0275-4.

Journel, A.G., (1986). Geostatistics: Models and tools for the earth sciences. *Mathematical Geology* 18(1): 119–140, https://doi.org/10.1007/BF00897658.

Chilès, J.P., Delfiner, P. (1999). *Geostatistics: Modeling Spatial Uncertainty*, New York, John Wiley & Sons.

Isaaks, E., Srivastava, R. (1989). *An Introduction to Applied Geostatistics*, Oxford University Press.

Goovaerts, P. (1997). *Geostatistics for Natural Resources Evaluation*, New York, Oxford University Press.

Firat, M., Gungor, M., (2007). River flow estimation using adaptive neuro fuzzy inference system. *Mathematics and Computers in Simulation* 75(3): 87–96, https://doi.org/10.1016/j.matcom.2006.09.003.

Pratihar, D.K. (2008). *Soft Computing*, Oxford, Alpha Science International Ltd.

Erdem, G., Sagir, C., Canoglu, M.C., Kurtulus, B., 2016. Comparison of Empirical Bayesian Kriging and Geo Anfis methods for interpolating hydraulic head in a karst alluvium, 8th IEMSS Congress, 10-14 July 2016, Toulouse, France.

Zadeh, L., (1965). Fuzzy sets. *Information and Control* 8(3): 338–353.

BRGM, Bureau de Recherches Géologiques et Minères, (2020). https://www.geoportail.gouv.fr/donnees/cartes-geologiques is retrieved, Accessed Date: 15.01.2020.

Demuth, H., Beale, M. (2003). *Neural Network Toolbox for Use with MATLAB*, USA, The MathWorks Inc.

Li, J., Heap, A.D., (2014). Spatial interpolation methods applied in the environmental sciences: A review. *Environmental Modelling & Software*, 53: 173-189, https://doi.org/10.1016/j.envsoft.2013.12.008.